PERGAMON

International Journal of Heat and Mass Transfer 42 (1999) 1047–1057

International Journal of HEAT and MASS TRANSFER

Free convection in oblique enclosures filled with a porous medium

A. C. Baytas[a,*], I. Pop[b]

[a] *Istanbul Technical University, Institute for Nuclear Energy 80626—Maslak, Istanbul, Turkey*
[b] *University of Cluj, Faculty of Mathematics, R-3400 Cluj, CP 253, Romania*

Received 23 April 1998

Abstract

Detailed numerical calculations are presented in this paper for the steady-state free convection within an inclined cavity filled with a fluid-saturated porous medium. The inclined walls are maintained at constant but different temperatures, while the horizontal walls are adiabatic. To simplify the effort in matching the grid mesh with the inclined walls of the cavity, the computational domain is mapped onto a rectangular shape cavity using a non-linear axis transformation. The governing equations (in the stream function and temperature formulation) are expressed in the new coordinate system and solved numerically using the ADI (Alternative Direction Implicit) finite-difference method. Flow and heat transfer characteristics (stream lines, isotherms and average Nusselt number) are investigated for a wide range of values of the Rayleigh number, inclined angle and cavity aspect ratio. The present solutions for a vertical cavity are compared with the known results from the open literature. It was found that these results are in very good agreement. We believe that these results serve as a reference against which other solutions for the present problem can be compared in the future.

Nomenclature

a cavity width
A aspect ratio, equation (10)
g acceleration due to gravity
k effective thermal conductivity of the porous medium
K permeability of the porous medium
L cavity length
$\mathbf{n}$ unit vector
Nu local Nusselt number
$\bar{N}u$ average Nusselt number
q_w wall heat flux
Ra Rayleigh number, equation (10)
t time
T fluid temperature
T_c temperature of the cold wall
T_h temperature of the hot wall
x, y Cartesian coordinates
X, Y transformed coordinates, equation (3).

Greek symbols
α effective thermal diffusivity of the porous medium
β coefficient of thermal expansion
ΔT temperature difference
ε prescribed error
θ dimensionless temperature, equation (7)
ν kinematic viscosity
ξ, η dimensionless variables, equation (7)
σ ratio of heat capacity of porous medium to that of fluid
τ dimensionless time, equation (7)
ϕ inclined angle
$\bar{\psi}$ stream function
ψ dimensionless stream function, equation (7).

1. Introduction

The subject of thermal convection in porous media has been studied extensively in recent years and the growing

* Corresponding author

0017–9310/98/$—see front matter
PII: S0017–9310(98)00208–7

volume of work devoted to this subject has been amply documented in the monographs by Nield and Bejan [1], and Ingham and Pop [2]. This interest has been motivated by its importance in many natural and industrial applications. Prominent among these applications are heat exchangers, solar power collectors, migration of moisture through air contained in fibrous insulation, energy efficient drying processes, underground spread of pollutants, grain storage, food processing, packed-bed catalytic reactors, flows in water-percolated soils, cooling of radioactive waste containers, to name just a few.

Free convection in a rectangular porous cavity, whose vertical walls are maintained at two different temperatures or heat fluxes and the horizontal walls are insulated, is a fundamental problem in thermal convection in porous media, which has received the attention of many investigations. Walker and Homsy [3], Bejan [4], Prasad and Kulacki [5], Beckermann et al. [6], Gross et al. [7], Lai and Kulacki [8], Manole and Lage [9] have contributed some important theoretical results to this problem. The problem is still of continuing theoretical interest because it provides a simple geometry on which numerical techniques may be tested, even though exact analytical solutions do not exist.

However, relatively little work has been done on the problem of free convection in an inclined rectangular enclosure filled with a porous medium. An overview of this problem has been documented in the review article by Caltagirone [10] and in other papers by Moya et al. [11], Vasseur et al. [12] and Shen et al. [13]. Unlike the porous rectangular cavity free convection flow problem, the flow in an inclined cavity is not as simple to determine because of the sloping walls. In general, the mesh nodes will not lie along the sloping walls and, as a result, from a programming and computational point of view, the effort required for determining the convective flow in an inclined enclosure increases significantly.

The present paper concerns a numerical study of the steady free convection flow in an oblique cavity filled with a homogeneous porous medium. Some flow and heat transfer characteristics are determined for a large range of inclination angles, Rayleigh numbers and aspect ratios. To do it, the computational domain is mapped onto a rectangular shape cavity using a nonlinear axis transformation as proposed by Liu and Guerra [14], and Facas and Mottioli [15]. The Darcy momentum and energy equations are solved numerically using the Alternating Direction Implicit (ADI) method proposed by Douglas and Peaceman [16] applied in the transformed coordinate system. Sample results of flow and heat transfer characteristics are presented in graphical and tabular forms. Such graphs and tables can serve as a reference against which other numerical solutions or experimental data can be compared in the future for such inclined cavities.

To the authors' best knowledge this general situation of free convection in oblique enclosures has not yet been investigated.

2. Basic equations

The problem under consideration is shown in Fig. 1(a). Two inclined isothermal walls at temperatures T_h (hot) and T_c (cold), and two adiabatic horizontal walls enclose a fluid-saturated porous medium. The enclosure is of width a, length L and is inclined at an angle ϕ with respect to the vertical plane. In the porous medium, Darcy's law is assumed to hold, the fluid is assumed to be a normal Boussinesq fluid and the inertial effects are neglected. Under these assumptions, the conservation equations for momentum (Darcy) and energy for unsteady two-dimensional free convection flow can be written as, see Nield and Bejan [1],

$$\frac{\partial^2\bar{\psi}}{\partial x^2}+\frac{\partial^2\bar{\psi}}{\partial y^2}=-\frac{gK\beta}{\nu}\frac{\partial T}{\partial x} \tag{1}$$

$$\sigma\frac{\partial T}{\partial t}+\frac{\partial\bar{\psi}}{\partial y}\frac{\partial T}{\partial x}-\frac{\partial\bar{\psi}}{\partial x}\frac{\partial T}{\partial y}=\alpha\left(\frac{\partial^2 T}{\partial x^2}+\frac{\partial^2 T}{\partial y^2}\right) \tag{2}$$

where x and y are the Cartesian coordinates measured in the horizontal and vertical directions, respectively, t is the time, g is the acceleration due to gravity, α and K are, respectively, the thermal diffusivity and permeability of the porous medium, β is the coefficient of thermal expansion and σ is the ratio of heat capacity of porous medium to that of fluid. The stream function $\bar{\psi}$ is defined in the usual way $u=\partial\bar{\psi}/\partial y$ and $v=-\partial\bar{\psi}/\partial x$.

In general, no rectangular grid mesh can be generated that fits all four surfaces. However, the computational domain can be mapped onto a rectangular domain, as shown in Fig. 1(b), by using the following transformation, used also by Lin and Guerra [14] and Facas and Mottioli [15],

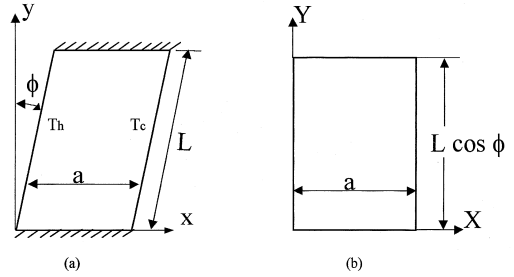

Fig. 1. (a) Physical model and coordinate system. (b) Transformed computational domain.

$$X = x - y\tan\phi, \quad Y = y. \tag{3}$$

Note that using this transformation one has

$$\frac{\partial}{\partial x} = \frac{\partial}{\partial X}, \quad \frac{\partial}{\partial y} = \frac{\partial}{\partial Y} - \tan\phi\frac{\partial}{\partial X}. \tag{4}$$

With (3) and (4), equations (1) and (2) became

$$\frac{\partial^2\bar{\psi}}{\partial X^2} - 2\sin\phi\cos\phi\frac{\partial^2\bar{\psi}}{\partial X\partial Y} + \cos^2\phi\frac{\partial^2\bar{\psi}}{\partial Y^2} = -\frac{gK\beta}{v}\cos^2\phi\frac{\partial T}{\partial X} \tag{5}$$

$$\sigma\frac{\partial T}{\partial t} + \frac{\partial\bar{\psi}}{\partial y}\frac{\partial T}{\partial x} - \frac{\partial\bar{\psi}}{\partial x}\frac{\partial T}{\partial y} = \frac{\alpha}{\cos^2\phi} \times\left(\frac{\partial^2 T}{\partial X^2} - 2\sin\phi\cos\phi\frac{\partial^2 T}{\partial X\partial Y} + \cos^2\phi\frac{\partial^2 T}{\partial Y^2}\right). \tag{6}$$

Further, we introduce the following dimensionless variables

$$\xi = X/a, \quad \eta = Y/(L\cos\phi), \quad \tau = t(\alpha/\sigma aL\cos\phi), \quad \psi = \bar{\psi}/\alpha, \quad \theta = (T - T_r)/\Delta T \tag{7}$$

where $T_r = (T_h + T_c)/2$ is a reference temperature and $\Delta T = T_h - T_c$ with $T_h > T_c$. Expressed in these variables, equations (5) and (6) transform to

$$\frac{\partial^2\psi}{\partial\xi^2} - 2\frac{\sin\phi}{A}\frac{\partial^2\psi}{\partial\xi\partial\eta} + \frac{1}{A^2}\frac{\partial^2\psi}{\partial\eta^2} = -Ra\cos^2\phi\frac{\partial\theta}{\partial\xi} \tag{8}$$

$$\frac{\partial\theta}{\partial\tau} + \frac{\partial\psi}{\partial\eta}\frac{\partial\theta}{\partial\xi} - \frac{\partial\psi}{\partial\xi}\frac{\partial\theta}{\partial\eta} = \frac{A}{\cos\phi} \times\left(\frac{\partial^2\theta}{\partial\xi^2} - 2\frac{\sin\phi}{A}\frac{\partial^2\theta}{\partial\xi\partial\eta} + \frac{1}{A^2}\frac{\partial^2\theta}{\partial\eta^2}\right) \tag{9}$$

where A is the cavity aspect ratio and Ra is the Rayleigh number which are defined as

$$A = L/a, \quad Ra = gK\beta\Delta Ta/(\alpha v). \tag{10}$$

Using (4) and (7), the relevant hydrodynamic and thermal boundary conditions of equations (8) and (9) can be written as

$$\psi = 0, \quad \theta = \frac{1}{2} \quad \text{on } \xi = 0$$

$$\psi = 0, \quad \theta = -\frac{1}{2} \quad \text{on } \xi = 1$$

$$\psi = 0, \quad \frac{\partial\theta}{\partial\eta} - A\sin\phi\frac{\partial\theta}{\partial\xi} = 0 \quad \text{on } \eta = 0, 1. \tag{11}$$

The problem is to find the functions ψ and θ which satisfy the governing equations (8) and (9), and boundary conditions (11). The solution of this problem is dependent on the parameters A, Ra and ϕ.

Having determined ψ and θ, we can evaluate the heat fluxes from the oblique walls

$$q_w = -k\mathbf{n}\cdot\nabla T \tag{12}$$

where k is the thermal conductivity of the porous medium and $\mathbf{n}$ is the unit vector normal to the oblique walls

$$\mathbf{n} = \{-\cos\phi, \sin\phi\}. \tag{13}$$

Using (7), (12) and (13) we can express q_w as

$$q_w = -\frac{k\Delta T}{(a\cos\phi)}\left(\frac{\sin\phi}{A}\frac{\partial\theta}{\partial\eta} - \frac{\partial\theta}{\partial\xi}\right)_{\xi=0,1}. \tag{14}$$

The local Nusselt number, which is defined as

$$Nu(\xi,\eta) = \frac{aq_w}{k\Delta T} \tag{15}$$

then becomes

$$Nu(\xi,\eta) = -\frac{1}{\cos\phi}\left(\frac{\sin\phi}{A}\frac{\partial\theta}{\partial\eta} - \frac{\partial\theta}{\partial\xi}\right)_{\xi=0,1}. \tag{16}$$

Finally, the average Nusselt number is given by

$$\bar{Nu}(\xi) = \int_0^1 Nu(\xi,\eta)\,d\eta. \tag{17}$$

3. Results and discussion

The coupled equations (8) and (9) along with the boundary conditions (11) are solved numerically using the Alternating Direction Implicit (ADI) method developed by Douglas and Peaceman [16] for heat flow problems and adapted by Wilkes and Churchill [17] for natural convection in enclosures. The method leads to three diagonal systems of simultaneous equations that are much easier to solve than the penthadiagonal systems, which arise when fully implicit methods are used. The iteration process is terminated when the following criterion is satisfied

$$\sum_{i,j}|\chi_{i,j}^{n+1} - \chi_{i,j}^{n}| \Big/ \sum_{i,j}|\chi_{i,j}^{n+1}| \leqslant \varepsilon \tag{18}$$

where χ stands for ψ or θ; n denotes the iteration order and ε is a prescribed error ($\varepsilon = 10^{-5}$). A good description of this method is given in Baytas [18–20] and it is unnecessary to repeat the details here.

Numerical results were obtained for a cavity with an aspect ratio $A = 0.7$, 0.9 and 1.0 (square cavity) when the inclination angle $\phi = 0^\circ$, $\pm 15^\circ$, $\pm 30^\circ$, $\pm 45^\circ$ and $\pm 60^\circ$. The values covered for the Rayleigh number are $Ra = 10$, 100, 1000, 5000 and 10 000. Tables 1 and 2 compare the accuracy of the average Nusselt number $\overline{Nu}$ for $A = 1.0$ and $\phi = 0^\circ$ (vertical enclosure), with $A = 0.7$ and 0.9, and different values of the Rayleigh number with some numerical solutions reported by different authors. It is seen from these tables that the agreement between the present and the previous results

Table 1
Comparison of $\overline{Nu}$ for $A = 1$ and $\phi = 0^\circ$ with some previous numerical results

	Ra			
Authors	10	100	1000	10 000
Walker and Homsy [3]		3.097	12.96	51
Bejan [4]		4.2	15.8	50.80
Beckerman et al. [6]		3.113		48.9
Gross et al. [7]		3.141	13.448	42.583
Manole and Lage [9]		3.118	13.637	48.117
Moya et al. [11]	1.065	2.801		
Present results	1.079	3.16	14.06	48.33

Table 2
Comparison of $\overline{Nu}$ for $\phi = 0^\circ$ with some previous numerical results

	Ra			
	1000		5000	
A	Prasad and Kulacki [5]	Present results	Prasad and Kulacki [5]	Present results
0.7	13.51	10.13	38.95	34.24
0.9	14.19	12.27	35.49	31.86

is very good. Therefore, we are confident that the results presented in this paper are very accurate.

The combined effects of inclination and Rayleigh number on the fluid flow patterns (streamlines and isotherms) are illustrated in Figs 2–6. It is seen from these figures that isotherms (left) are equally spaced between the maximum temperature of the hot wall and the minimum temperature of the cold wall. The streamlines (right) are also equally spaced with specified increment between a value of zero on the boundaries and the extreme value ψ_{max}. It is worth mentioning that the results for the vertical square cavity ($\phi = 0^\circ$) compare very well with those of Prasad and Kulacki [5]. Further, we see that a sufficiently large value of the Rayleigh number ($Ra = 10^4$) causes a boundary layer flow in which the dominant mode of heat transfer is convection. This can be seen more clearly in Fig. 2(b). Then, Figs 2(b)–6(b) show that the flow field comprises a primary cell of relatively high velocity, circulating around the entire enclosure. This cell becomes smaller as ϕ increases. A cell also arises for the temperature field at a sharper corner, as can be seen from Fig. 5(d) left. However, Fig. 6(d) left indicate that two cells occur at $\phi = -60^\circ$ due to the much lower velocity prevailing at that corner and they occupy nearly half of the cavity area.

Values of the local Nusselt number *Nu* on the left and right walls of the square cavity ($A = 1$) are plotted in Fig. 7 against the dimensionless coordinate η for $Ra = 10^3$. Figure 7(a) shows the variation of *Nu* for $\phi = 45^\circ$ and Fig. 7(b) is for $\phi = -45^\circ$. It can be seen from Fig. 7(a) that on the hot wall *Nu* first increases and then decreases taking a minimum value near the top wall of the cavity. This is because of lower convective velocity on the top wall. However, on the cold wall, *Nu* first decreases and then increases and reaches its maximum value near the top wall. In contrast, Fig. 7(b) shows that on the hot wall, *Nu* decreases monotonically from its maximum value near the bottom side to zero near the topside. But, *Nu* at the cold wall increases monotonically from zero at the bottom side to a maximum value at the topside of the wall. This is consistent with the observed higher convective flow in the upper and lower corners of the cavity, as can be seen from Figs 2–6.

Finally, Fig. 8 illustrates the variation of the average Nusselt number $\overline{Nu}$ at the hot (left) wall of the square cavity ($A = 1.0$) when $Ra = 100$, 1000 and 10 000. As expected, *Nu* increases as *Ra* is increased. It is also seen that $\overline{Nu}$ decreases almost linearly for relatively low values of *Ra* but, as *Ra* increases to 10 000, the variation of $\overline{Nu}$ deviates from its linear variation.

4. Conclusions

Steady-state flow and heat transfer characteristics have been investigated for the free convection flow in an inclined cavity filled with a porous medium. With numerical integration of the complete set of couplet partial differential equations, based on time ADI method, we have been able to confirm the stable steady-state solutions, obtaining very good agreement with known results from the open literature. However, computations are increasingly difficult as ϕ increases. The results show that near the sharp corners of the cavity the flow and temperature break down into a series of subvortices. The subvortex system grows in size with increased inclination and Rayleigh number.

We hope to report further results on this problem soon, especially as regards to other values of the parameter *A*.

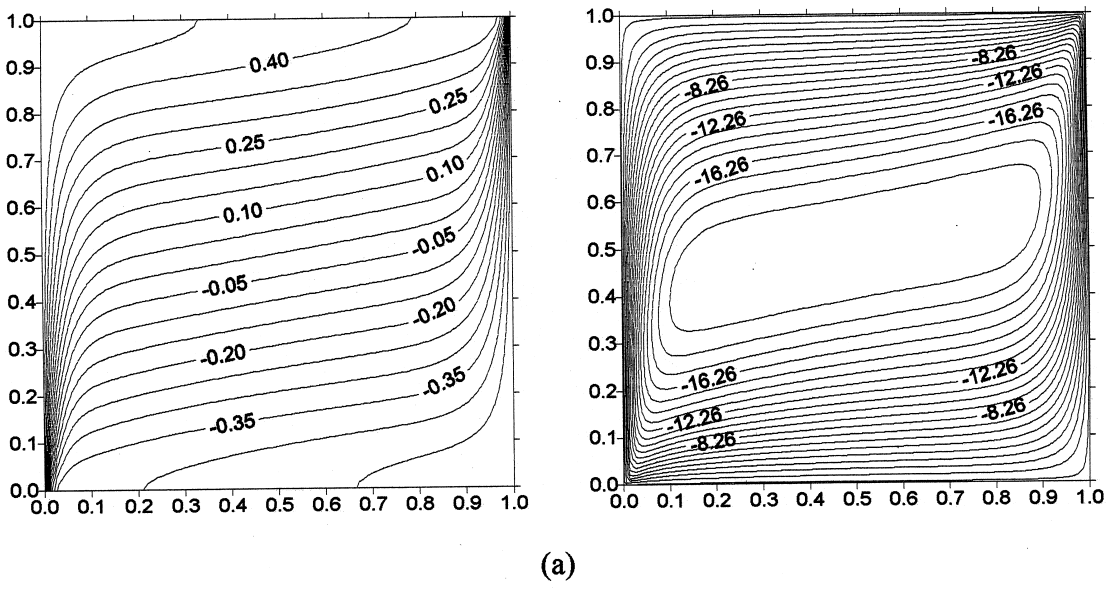

Fig. 2. Isotherms and streamlines for $A = 1.0$ and $\phi = 0^{\circ}$; (a) $Ra = 10^3$, (b) $Ra = 10^4$.

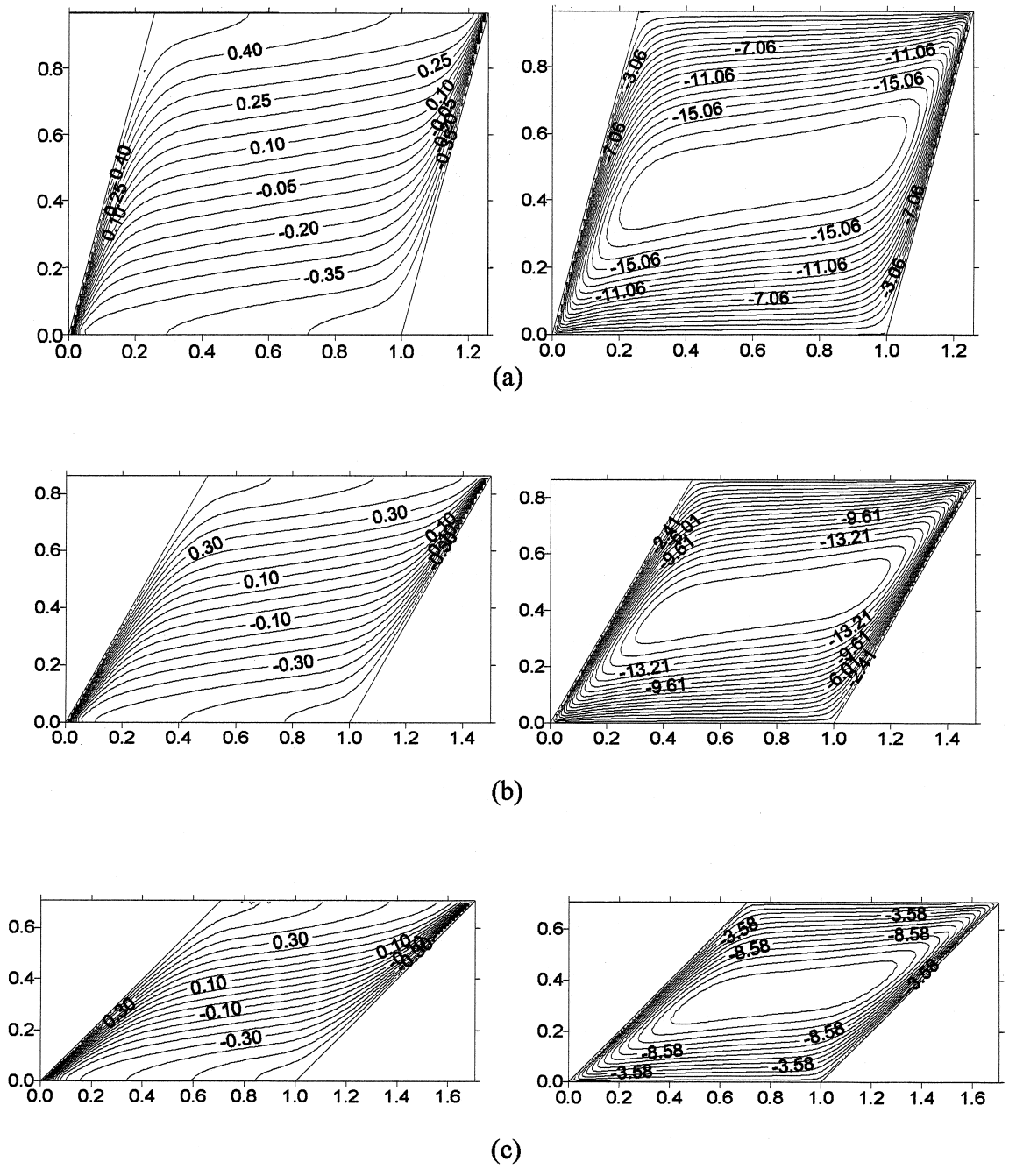

Fig. 3. Isotherms and streamlines for $A = 1.0$ and $Ra = 10^3$; (a) $\phi = 15^\circ$, (b) $\phi = 30^\circ$, (c) $\phi = 45^\circ$.

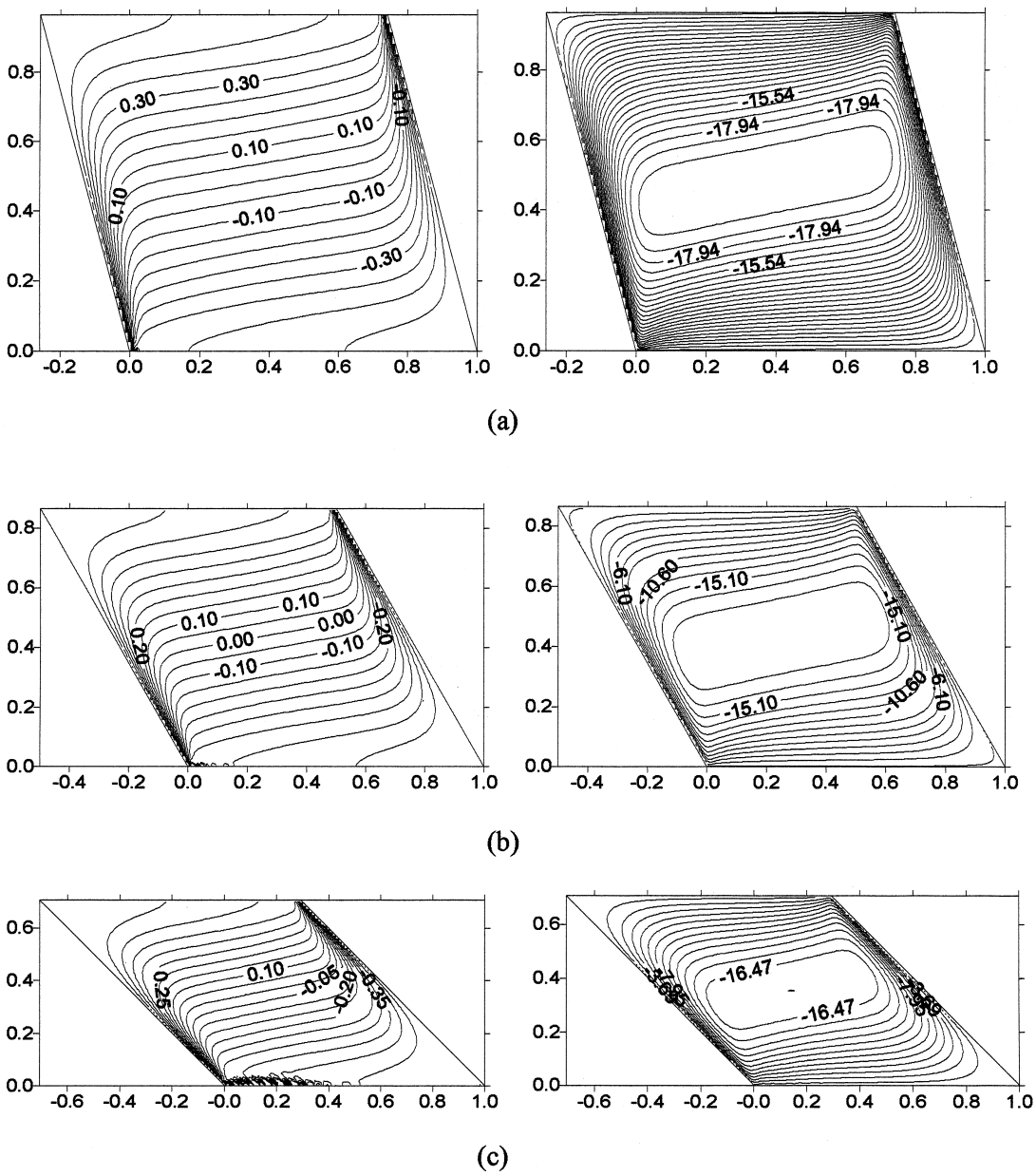

Fig. 4. Isotherms and streamlines for $A = 1.0$ and $Ra = 10^3$; (a) $\phi = -15^\circ$, (b) $\phi = -30^\circ$, (c) $\phi = -45^\circ$.

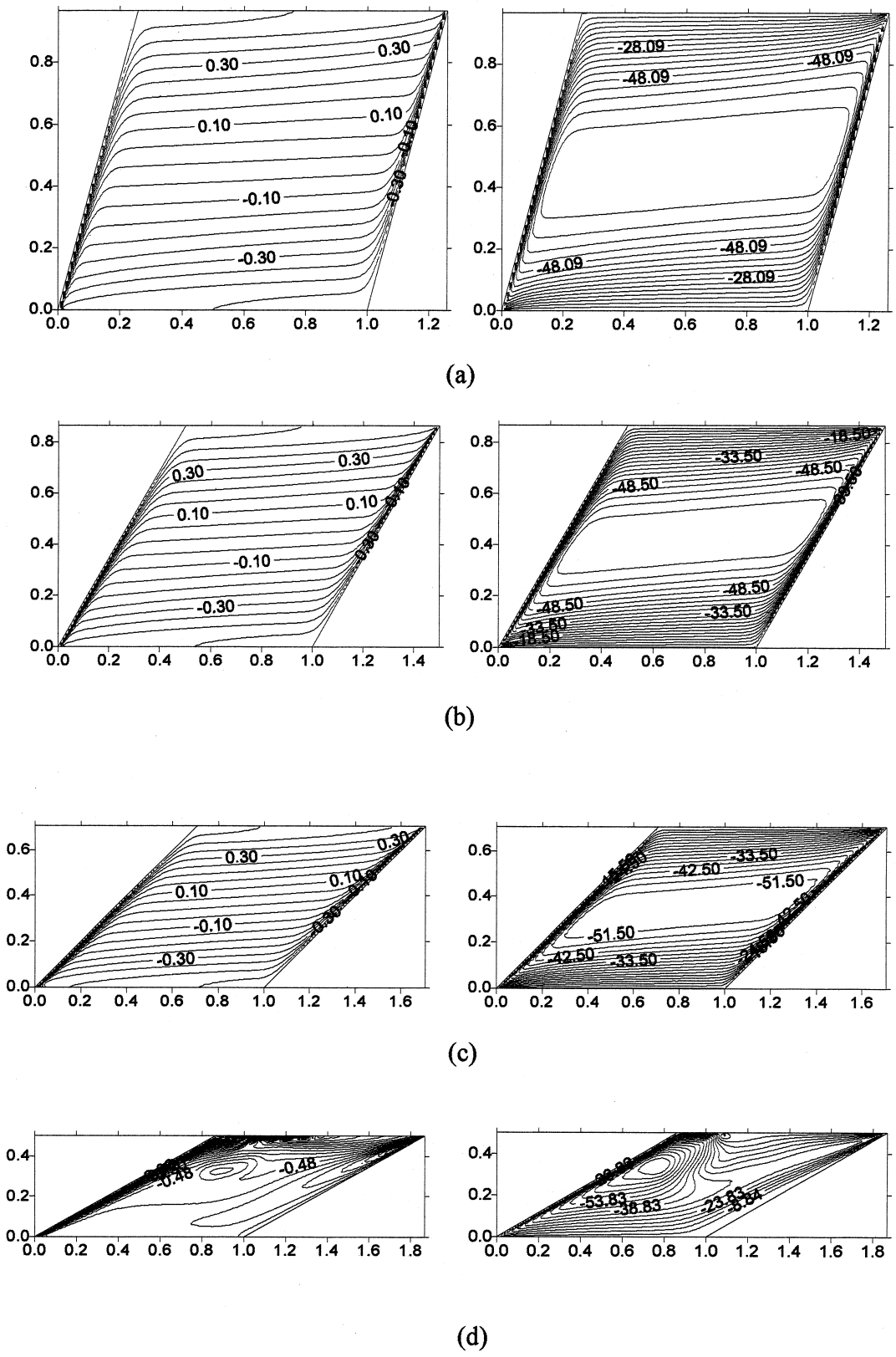

Fig. 5. Isotherms and streamlines for $A = 1.0$ and $Ra = 10^4$; (a) $\phi = 15°$, (b) $\phi = 30°$, (c) $\phi = 45°$, (d) $\phi = 60°$.

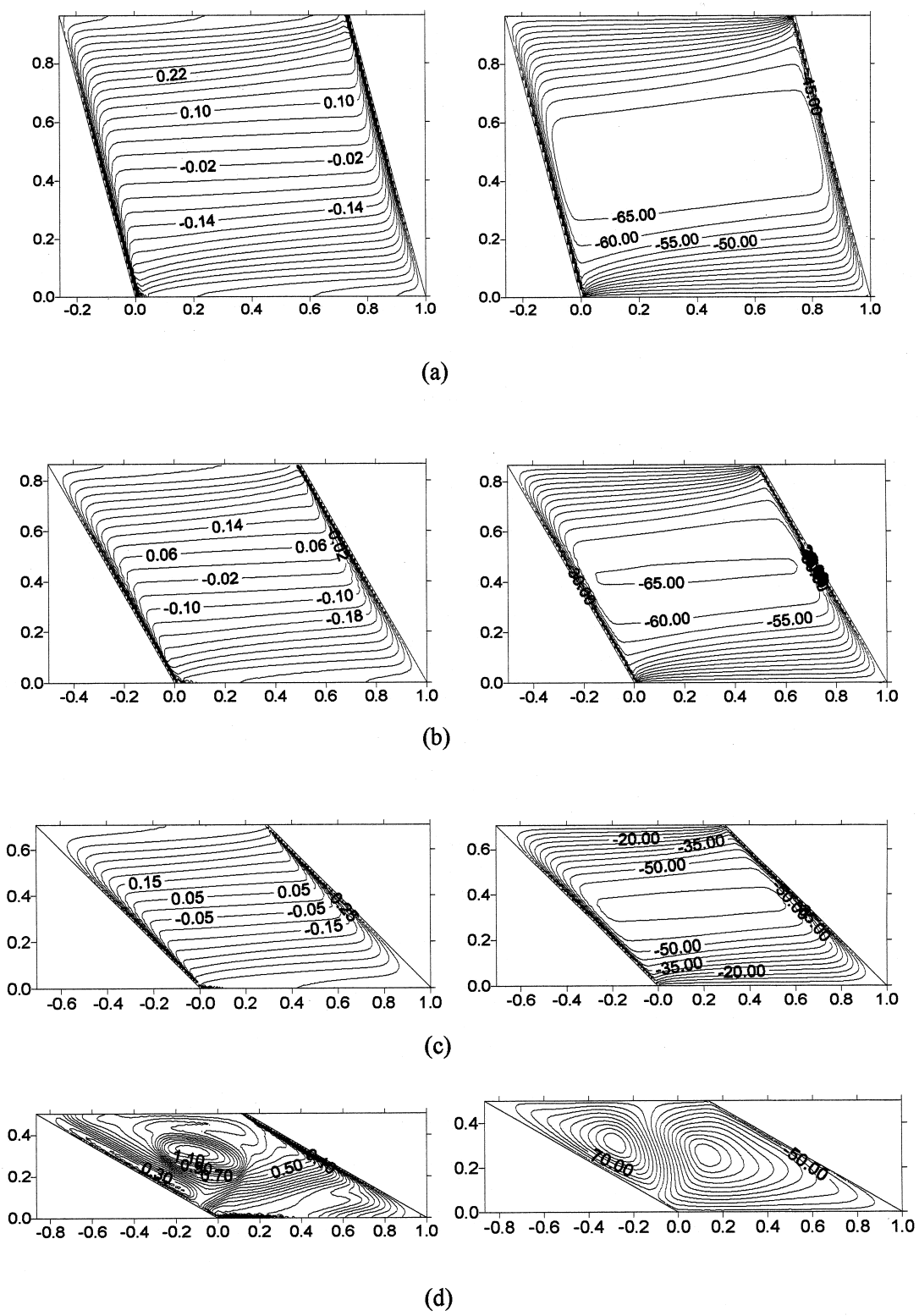

Fig. 6. Isotherms and streamlines for $A = 1.0$ and $Ra = 10^4$; (a) $\phi = -15^\circ$, (b) $\phi = -30^\circ$, (c) $\phi = -45^\circ$, (d) $\phi = -60^\circ$.

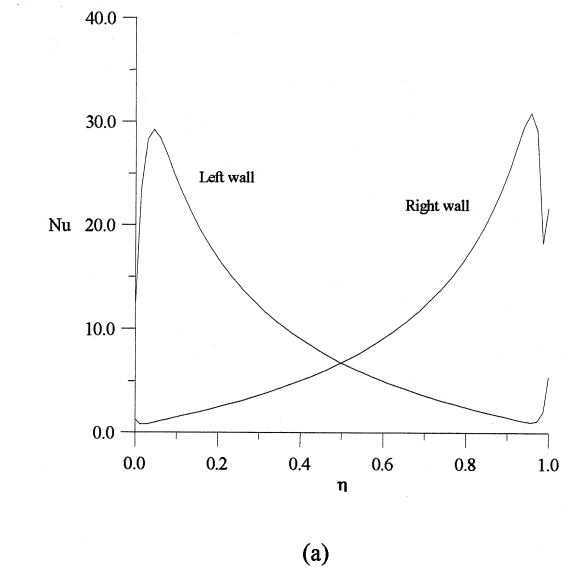

Fig. 7. Variation of Nu with η for $Ra = 10^3$ and $A = 1.0$; (a) $\phi = 45°$, (b) $\phi = -45°$.

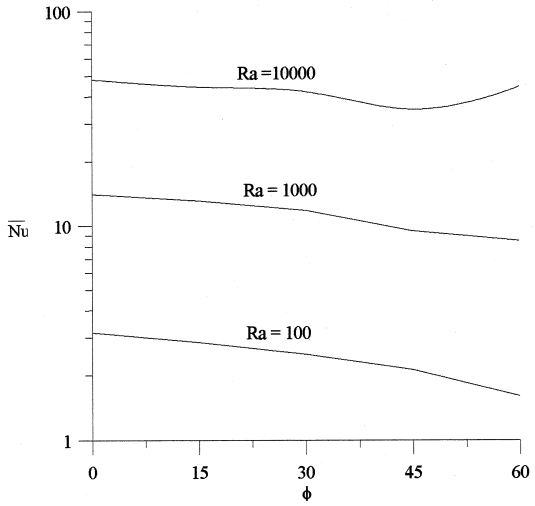

Fig. 8. Variation of $\overline{Nu}$ on the hot wall with ϕ for $A = 1.0$ when $Ra = 100$, 1000 and 10 000.

References

[1] D.A. Nield, A. Bejan, Convection in Porous Media, Springer, New York, 1992.
[2] D.B. Ingham, I. Pop (Eds.), Transport Phenomena in Porous Media, Elsevier, Amsterdam, 1998.
[3] K.L. Walker, G.M. Homsy, Convection in a porous cavity, J. Fluid Mech. 87 (1978) 449–474.
[4] A. Bejan, On the boundary layer regime in a vertical enclosure filled with a porous medium, Lett. Heat Mass Transfer 6 (1979) 93–102.
[5] V. Prasad, F.A. Kulacki, Convective heat transfer in a rectangular porous cavity—effect of aspect ratio on flow structure and heat transfer, J. Heat Transfer 106 (1984) 158–165.
[6] C. Beckermann, R. Viskanta, S. Ramadhyani, A numerical study of non-Darcian natural convection in a vertical enclosure filled with a porous medium, Num. Heat Transfer 10 (1986) 557–570.
[7] R.J. Gross, M.R. Bear, C.E. Hickox, The application of flux-corrected transport (FCT) to high Rayleigh number natural convection in a porous medium, in: Proc. 8th Int. Heat Transfer Conf., San Francisco, CA, 1986.
[8] F.C. Lai, F.A. Kulacki, Natural convection across a vertical layered porous cavity, Int. J. Heat Mass Transfer 31 (1988) 1247–1260.
[9] D.M. Manole, J.L. Lage, Numerical benchmark results for natural convection in a porous medium cavity, HTD-Vol. 216, Heat and Mass Transfer in Porous Media, ASME Conference 1992, pp. 55–60.
[10] J.-P. Caltagirone, Convection in a porous medium, in: J. Zierep, H. Oertel (Eds.), Convective Transport and Instability Phenomena, G. Braun, Karlsruhe, 1982, pp. 192–232.
[11] S.L. Moya, E. Ramos, M. Sen, Numerical study of natural convection in a tilted rectangular porous material, Int. J. Heat Mass Transfer 30 (1987) 741–756.
[12] P. Vasseur, M.G. Satish, L. Robillard, Natural convection in a thin inclined porous layer exposed to a constant heat flux, Int. J. Heat Mass Transfer 30 (1987) 537–549.
[13] M. Sen, P. Vasseur, L. Robillard, Multiple steady states for unicellular natural convection in an inclined porous layer, Int. J. Heat Mass Transfer 30 (1987) 2097–2113.
[14] C.Y. Liu, A.C. Guerra, Free convection in a porous medium near the corner of arbitrary angle formed by two vertical plates, Int. Comm. Heat Mass Transfer 12 (1985) 431–440.
[15] G.N. Facas, T. Mottioli, A numerical study of viscous flow in an inclined cavity, in: M.A. Ebadian, D.W. Pepper, T.

Diller (Eds.), Advances in Heat Transfer Augmentation and Mixed Convection, ASME 1991, HTD-169, pp. 5–12.
[16] J.Jr. Douglas, D.W. Paceman, Numerical solution of two-dimensional heat flow problems. A.I.Ch.E. J. 1 (1955) 502–512.
[17] J.O. Wilkes, S.W. Churchill, The finite difference computation of natural convection in a rectangular enclosure, A.I.Ch.E. J. 12 (1966) 161–166.
[18] A.C. Baytas, Buoyancy-driven flow in an enclosure containing time periodic internal sources, Heat and Mass Transfer 31 (1996) 113–119.
[19] A.C. Baytas, Transient natural convection and orientation optimization in a differentially heated inclined square enclosure with internal heat sources, in: J. Padet, F. Arinc (Eds.), ICHMT, International Symposium on Transient Convective Heat Transfer, 19–23 August 1996, Cesme, Turkey, Begel House, Inc., New York, 1997, pp. 117–125.
[20] A.C. Baytas, Optimization in an inclined enclosure for minimum entropy generation in natural convection, J. Non-Equil. Thermodyn. 22 (1997) 145–155.